The Transmitted Signals of OTFS and VOFDM Are Exactly the Same

Xiang-Gen Xia

University of Delaware

Newark, DE 19716, USA

Email: xxia@ee.udel.edu

April 25, 2022

Abstract

This short note connects OTFS and single transmit antenna VOFDM systems and explains why VOFDM is good to time varying channels with Doppler spread, which also explains why OTFS is so, as well.

Main Description

It is not hard to check that the transmitted signals in either discrete or continuous time format of OTFS [7] and single transmit antenna vector OFDM (VOFDM) [1, 2] are the same. For the discrete time format, for convenience, assume that the pulse g(t) is rectangular. Then, the transmitted sequences of OTFS and VOFDM are the same. If a more general continuous time pulse g(t) is used, the transmitted signal waveform of VOFDM is the same as that of OTFS, i.e., formula (5) in [7], no matter whether channel is stationary or time-varying. Note that the cyclic prefix for VOFDM does not have to be a multiple of vectors and it can be a truncated sequence of length not smaller than the channel length in order to have free interference across vector subchannels [4].

Recently it has been claimed that OTFS is good to deal with Doppler spread for time-varying channels [7]. From the VOFDM point of view, it has been shown in [1, 2, 3, 4] that VOFDM can achieve multipath diversity and/or signal space diversity, even with the MMSE linear receiver in a vectorized subchannel [4]. This is because in VOFDM, at transmit side, a vector of information symbols is DFT (or IDFT) transformed implicitly and then, at receive side, the information symbols in this vector are demodulated together. More specifically, since in VOFDM, a vectorized channel matrix is pseudo-circulant, it can be diagonalized by DFT/IDFT matrix with a phase shift diagonal matrix, see formula (4.1) in [2]. Then, this DFT (or IDFT) of a vector of information symbols is similar to the precoding in single antenna systems to collect signal space diversity to combat wireless fading (Doppler effect) [5] or diagonal space-time block coding in MIMO systems to collect spatial diversity [6]. This can be seen in [3] with a simplified demodulator as well. We believe that it is the main reason why OTFS (or VOFDM) is good to deal with a time-varying channel with both Doppler and time spreads.

In [10], a more general setting than VOFDM has been studied, where a channel independent precoder G, a matrix of size $M \times K$ with $K \leq M$, is used at the transmitter, where the precoder has K input information symbols and produces M output symbols to transmit. The simplest precoder studied in [10] is the identity matrix (or the $M \times K$ submatrix of the $M \times M$ identity matrix), and when

M = K, it is VOFDM. In [10], this general setting is studied for time-varying channels with both time and Doppler spreads (see the channel equation (7.4.1) on page 172 of [10]) in both theory and simulations (see Section 7.4 of [10] that is attached).

Furthermore, single transmit antenna VOFDM is a bridge between OFDM and single carrier frequency domain equalizer (SC-FDE) [4]. VOFDM converts an intersymbol interference (ISI) channel to multiple vectorized subchannels and there is no ISI across these vectorized subchannels. In each vectorized subchannel, the information symbols inside an information symbol vector may interfer each other, i.e., they may have ISI, but the length of ISI is limited to the vector size. When the vector size is 1 in VOFDM, it is OFDM. In this case, there is no ISI even in each subchannel. When the vector size is not less than a channel length and IFFT size is 1, it is SC-FDE. In this case, the length of ISI is the same as the length of the ISI channel.

For more details about single transmit antenna VOFDM, please see [2], [4]. For quasi-static channels (or stationary channels), it has been already shown in [8], [9] that OTFS is equivalent to VOFDM. Since quasi-static channel is arbitrary, when it is the ideal channel, i.e., $\delta(t)$, this equivalence also implies that the transmitted signals of OTFS and VOFDM are equivalent.

References

[1] X.-G. Xia, "Precoded OFDM systems robust to spectral null channels and vector OFDM systems with reduced cyclic prefix length," *Proceedings of ICC*, vol. 2, pp. 1110-1114, New Orleans, LA, USA, Jun. 18-22, 2000.

[2] X.-G. Xia, "Precoded and vector OFDM robust to channel spectral nulls and with reduced cyclic prefix length in single transmit antenna systems," *IEEE Trans. on Commun.*, vol. 49, no. 8, pp. 1363–1374, Aug. 2001.

[3] H. Zhang and X.-G. Xia, "Iterative decoding and demodulation for single antenna vector OFDM systems," *IEEE Trans. on Vehicular Technology*, vol. 35, no. 4, pp. 1447-1454, Jul. 2006.

[4] Y. Li, I. Ngebani, X.-G. Xia, and A. Host-Madsen, "On performance of vector OFDM with linear receivers," *IEEE Trans. on Signal Processing*, vol. 60, no. 10, pp.5268-5280, Oct. 2012.

[5] J. Boutros and E. Viterbo, "Signal space diversity: a power- and bandwidth-efficient diversity technique for the Rayleigh fading channel," *IEEE Trans. on Inform. Theory*, vol. 44, pp. 1453-1467, Jul. 1998.

[6] M. O. Damen, K. A. Meraim, and J.-C. Belfiore, "Diagonal algebraic space-time block codes," *IEEE Transactions on Information Theory*, vol. 48, pp. 628-636, Mar. 2002.

[7] R. Hadani, S. Rakib, M. Tsatsanis, A. Monk, A. J. Goldsmith, A. F. Molisch, and R. Calderbank, "Orthogonal time frequency space modulation," in *Proc. IEEE Wireless Commun. Netw. Conf. (WCNC)*, San Francisco, CA, USA, pp. 1-6, Mar. 2017.

[8] P. Raviteja, Y. Hong, and E. Viterbo, "OTFS performance on static multipath channels," *IEEE Wireless Commun. Lett*., vol. 8, no. 3, pp. 745 – 748, Mar. 2019.

[9] Y. Ge, Q. Deng, P. C. Ching, and Z. Ding, "OTFS signaling for uplink NOMA of heterogeneous mobility users," *IEEE Trans. on Commun*., vol. 69, no. 5, pp. 3147-3161, May 2021.

[10] X.-G. Xia, *Modulated Coding for Intersymbol Interference Channels*, New York, Marcel Dekker, Oct. 2000.

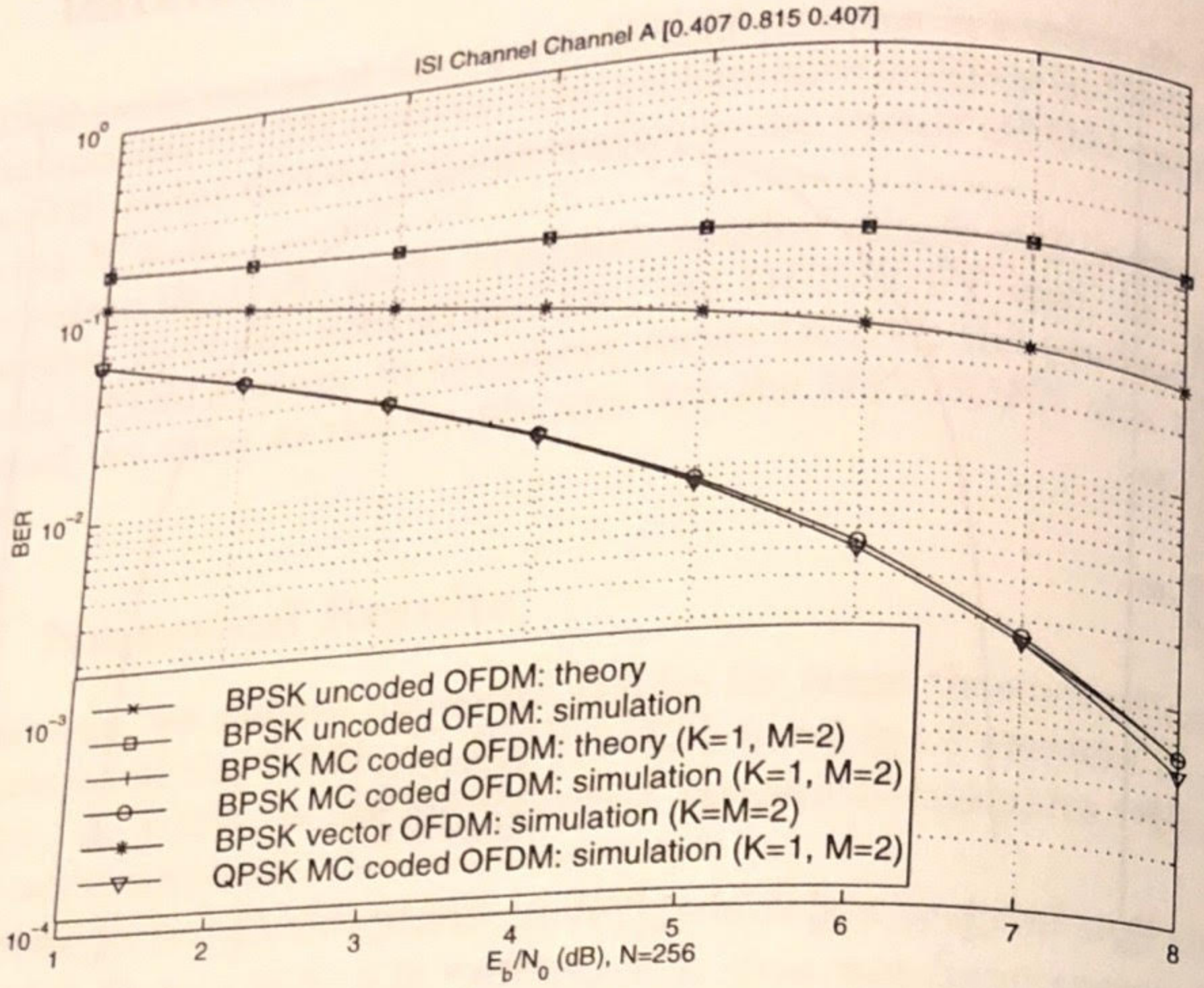

Figure 7.6: Performance comparison of OFDM systems: Channel A.

and $(256 + 10)/256$, respectively. Note that the prefix length of the vector OFDM system is only half of that of the conventional OFDM system.

7.4 Channel Independent MC Coded OFDM System for Frequency-Selective Fading Channels

In the previous sections, we studied the MC coded OFDM systems in time-invariant ISI channels. In this section, we want to study the performance of the MC coded OFDM systems in time-variant ISI channels, i.e., frequency-selective multipath fading channels, modeled as

$$y(n) = \sum_{l=0}^{L-1} h_l(n)x(n-l) + \eta(n), \tag{7.4.1}$$

where $x(n)$ and $y(n)$ are the input and output, respectively, and $\eta(n)$ is the additive noise as before, and L is the number of paths, i.e., the channel

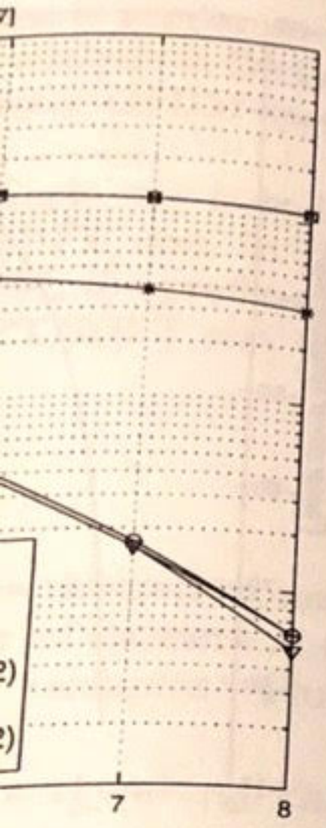

stems: Channel A.

length of the vector
OFDM system.

oded
y-Selective

M systems in time-
the performance of
els, i.e., frequency-

(7.4.1)

ively, and $\eta(n)$ is
, i.e., the channel

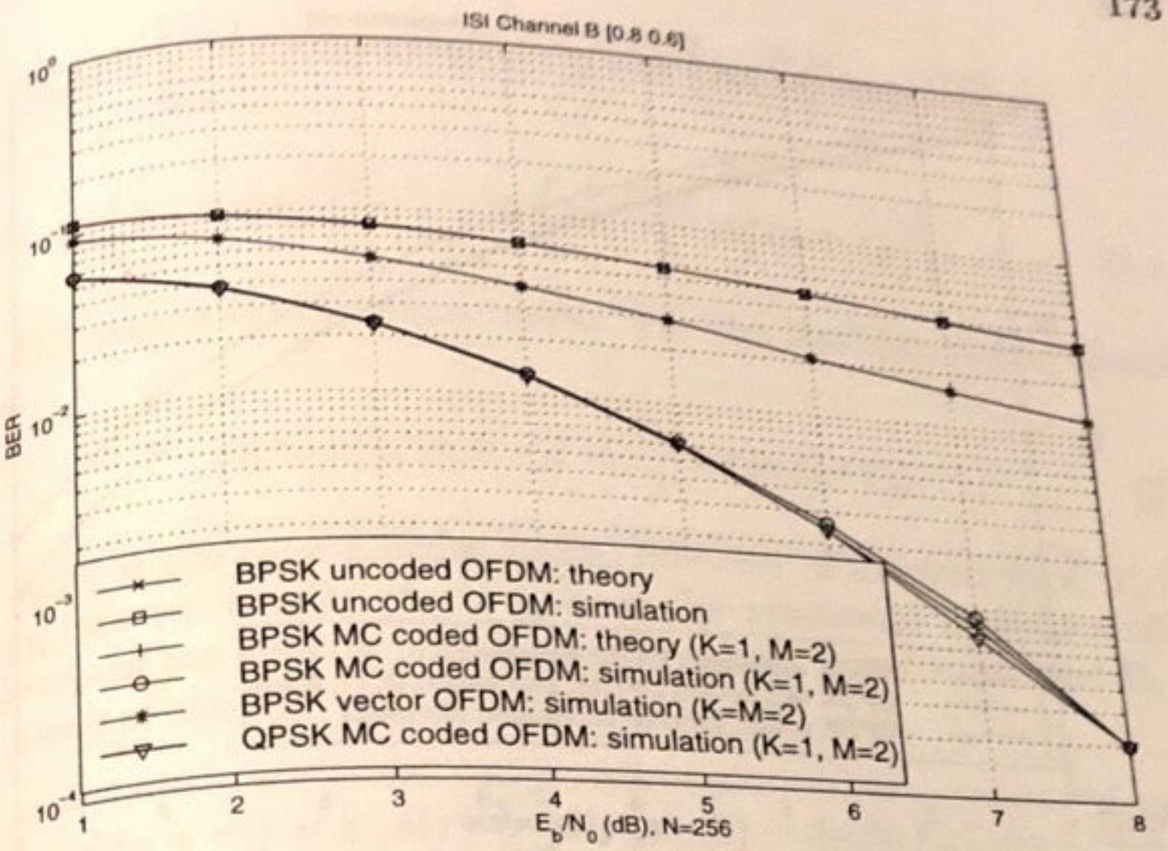

Figure 7.7: Performance comparison of OFDM systems: Channel B.

taps. We assume that the input information symbol sequence $x(n)$ is i.i.d. with mean 0 and variance E_x. We also assume that the multipaths h_l are independent of each other. The main idea of the following study is to approximate the time-variant $h_l(n)$ by using time-invariant paths in each MC coded OFDM block and move the approximation error into the additive noise, where the block length of the MC coded OFDM system in Fig.7.2 is NM, N is the number of subcarriers, i.e., the DFT length, and M is the block/vector length.

7.4.1 Performance Analysis

For convenience, we consider the frequency-selective multipath channel (7.4.1) in the block $n = 1, 2, ..., NM$ and use the center channel value $h_l(\frac{NM}{2})$ as the approximation value of $h_l(n)$, $n = 1, 2, ..., NM$, for each $l = 0, 1, ..., L-1$, and it is also used in the MC coded OFDM system decoding. Then, we have

$$y(n) = \sum_{l=0}^{L-1} h_l(\frac{NM}{2})x(n-l) + \eta_1(n) + \eta(n), \qquad (7.4.2)$$

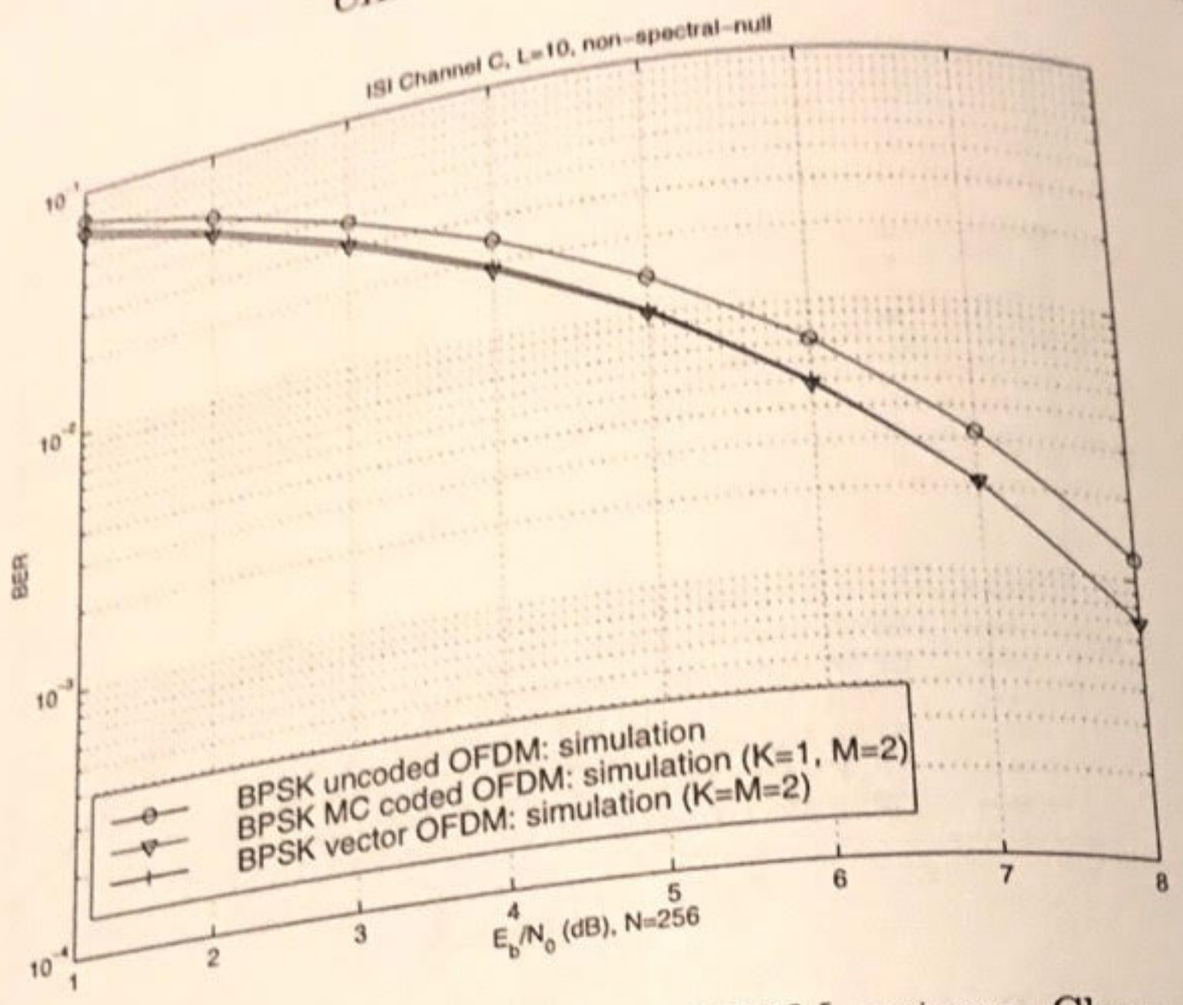

Figure 7.8: Performance comparison of OFDM systems: Channel C.

where

$$\eta_1(n) = \sum_{l=0}^{L-1} \left(h_l(n) - h_l(\frac{NM}{2}) \right) x(n-l) \tag{7.4.3}$$

is the approximation error of the multipath channel and independent of the additive noise $\eta(n)$. Thus, the MC coded OFDM system in the time-variant channel (7.4.1) becomes the one in the time-invariant channel (7.4.2) and at the receiver, the MC coded OFDM system becomes (7.2.15), where the constant matrices $\bar{\mathbf{H}}_k$ are from the time-invariant ISI channel $h_l = h_l(\frac{NM}{2})$, $l = 0, 1, ..., L-1$, and the additive noise is from the original $\eta(n)$ and the approximation error $\eta_1(n)$. Therefore, to study the performance, we only need to study the noise $\eta_1(n) + \eta(n)$ and the singular values of $\bar{\mathbf{H}}_k$ in the linear systems (7.2.15). Let us first study the noise $\eta_1(n)$ in (7.4.3). By the independence of h_l, $l = 0, 1, ..., L-1$, and the i.i.d. property of the input $x(n)$, the correlation function $\eta_1(n)$ is

$$E\left(\eta_1(n)\eta_1^*(n+\tau)\right) =$$

$$E_x\delta(\tau)\sum_{l=0}^{L-1}\Big[E\left(h_l(n)h_l^*(n-\right.$$

$$-E\left(h_l(n)h_l^*(\frac{NM}{2})\right)-$$

where $E(\cdot)$ stands for the expec
we have

$$E(h_l(n)h_l^*(n$$

where $J_0(x)$ is the zeroth-ord
sampling interval length, f_m
the velocity of the mobile us
mean power of the lth path

$$E(\eta_1(n)\eta_1^*(n+\tau)) = E_x\delta$$

Thus, the mean power of

$$\sigma_{\eta_1}^2 = \frac{\sum_{n=1}^{NM}\sum_{l=0}^{L-}}{}$$

and the total mean noi

After the mean no
systems (7.2.15) at t
the SVD decomposi
system:

$$\tilde{y}_k(n) = \Lambda_k($$

where $V_k(n)$ are K
of the form

and $\lambda_1, \lambda_2, ...,$

$$E_x\delta(\tau)\sum_{l=0}^{L-1}\left[E\left(h_l(n)h_l^*(n+\tau)\right)+E\left(h_l(\frac{NM}{2})h_l^*(\frac{NM}{2})\right)\right.$$

$$\left.-E\left(h_l(n)h_l^*(\frac{NM}{2})\right)-E\left(h_l(\frac{NM}{2})h_l^*(n+\tau)\right)\right], \qquad (7.4.4)$$

where $E(\cdot)$ stands for the expectation. For the Rayleigh fading channels, we have

$$E(h_l(n)h_l^*(n+\tau))=\frac{\Omega_l}{2}J_0(2\pi f_m\tau T_s), \qquad (7.4.5)$$

where $J_0(x)$ is the zeroth-order Bessel function of the first kind, T_s is the sampling interval length, $f_m=v/\lambda_c$ is the maximum Doppler shift, v is the velocity of the mobile user, λ_c is the carrier wavelength, and Ω_l is the mean power of the lth path h_l. Thus,

$$E(\eta_1(n)\eta_1^*(n+\tau))=E_x\delta(\tau)\sum_{l=0}^{L-1}\Omega_l\left(J_0(0)-J_0(2\pi f_mT_s(n-\frac{NM}{2}))\right). \qquad (7.4.6)$$

Thus, the mean power of η_1 is

$$\sigma_{\eta_1}^2=\frac{\sum_{n=1}^{NM}\sum_{l=0}^{L-1}\Omega_l\left(J_0(0)-J_0(2\pi f_mT_s(n-\frac{NM}{2}))\right)}{NM}, \qquad (7.4.7)$$

and the total mean noise power is

$$\sigma_{\eta_1}^2+\sigma_\eta^2. \qquad (7.4.8)$$

After the mean noise power is calculated, we now come back to the linear systems (7.2.15) at the receiver with respect to the channel (7.4.2). Using the SVD decomposition of $\bar{\mathbf{H}}_k$, (7.2.15) becomes the following equivalent system:

$$\tilde{y}_k(n)=\Lambda_k(n)V_k(n)\bar{x}_k(n)+\tilde{\xi}_k(n),\ \ k=0,1,...,N-1, \qquad (7.4.9)$$

where $V_k(n)$ are $K\times K$ unitary matrices, and $\Lambda_k(n)$ are $M\times K$ matrices of the form

$$\Lambda_k(n)=\begin{bmatrix}\mathrm{diag}(\lambda_1,...,\lambda_K)\\ 0_{(M-K)\times K}\end{bmatrix}, \qquad (7.4.10)$$

and $\lambda_1,\lambda_2,...,\lambda_K$ are K nonzero singular values of $\bar{\mathbf{H}}_k$.

For convenience, in what follows we consider BPSK signaling, i.e., $\tilde{x}_k(n)$ take binary values. When $K = 1$, the BER of (7.4.9) is

$$P_e = \int Q\left(\sqrt{\frac{\lambda^2 E_b}{\sigma_{\eta_1}^2 + \sigma_\eta^2}}\right) p(\lambda) d\lambda, \tag{7.4.11}$$

where Q stands for the Q function, $E_b = E_x$ is the mean signal power per bit, and $p(\lambda)$ is the probability density function of the singular values λ_k in (7.4.10) and shall be estimated later. By taking the bandwidth expansion of the cyclic prefix insertion into account, the BER of the MC coded OFDM system in Fig.7.2 when $K = 1$, is

$$P_b = \int Q\left(\sqrt{\frac{\lambda^2 E_b N}{(\sigma_{\eta_1}^2 + \sigma_\eta^2)(N + \tilde{\Gamma})}}\right) p(\lambda) d\lambda. \tag{7.4.12}$$

When $K > 1$, although it is hard to have the exact BER expression due to the fact that the K noise components in (7.4.9) after the inversion of the matrix $V_k(n)$ may not be i.i.d., it is not hard to derive its lower and upper bounds as follows. The BER is lower bounded by the BER when all the K noise components in $(V_k(n))^{-1}\tilde{\xi}_k(n)$ are i.i.d., i.e.,

$$P_b \geq \int Q\left(\sqrt{\frac{E_b K N}{\gamma(\sigma_{\eta_1}^2 + \sigma_\eta^2)(N + \tilde{\Gamma})}}\right) p(\gamma) d\gamma, \tag{7.4.13}$$

where γ is determined by the singular values λ_k in (7.4.10) as

$$\gamma = \sum_{k=1}^{K} \frac{1}{\lambda_k^2}, \tag{7.4.14}$$

and $p(\gamma)$ is the probability density function of random variable γ. The BER is upper bounded by the BER when the total noise power of all the components is in one of the K noise components in $(V_k(n))^{-1}\tilde{\xi}_k(n)$, i.e.,

$$P_b \leq \frac{1}{K} \int Q\left(\sqrt{\frac{E_b N}{\gamma(\sigma_{\eta_1}^2 + \sigma_\eta^2)(N + \tilde{\Gamma})}}\right) p(\gamma) d\gamma, \tag{7.4.15}$$

where γ is as in (7.4.14).

We next want to study the probability distribution of the singular values of the $\bar{\mathbf{H}}_k$ in (7.2.15) when $h_l = h_l(\frac{NM}{2})$ and $h_l(n)$ are Rayleigh fading. The distributions of the singular values can be determined as follows, when $K = N$ or $K = 1$.

Theorem 7.1 *The distributi system, i.e., $K = N$, in frequ nels is Rayleigh distribution.*

Proof. The blocked cha ization (2.3.10). By (7.2.9), $\mathbf{H}_k$ are the magnitudes of H Since each coefficient $h_l(\frac{N}{}$ variables $H(zW_M)|_{z=\exp(j}$ Gaussian. This proves Th Notice that when $M =$ and therefore, the singula have the Rayleigh distrib

Theorem 7.2 *The distr system with $K = 1$ in f nels is Nakagami distrib*

Proof. From the p $\mathbf{H}_k$ are all complex G are the norms of the t Nakagami distribution For the MC codec the distribution of the distributions from ou in Section 7.4.2 and Since, the BER b and its probability though we are not $K > 1$, our many distribution from t gamma distributio

7.4.2 Simula

We now present s in Fig.7.2 in frec two ray Rayleigh Ω_2. Each Rayle with the followi components, 8 c sample interval

we consider BPSK signaling, i.e., $\tilde{x}_k(n)$
e BER of (7.4.9) is

$$\left.\frac{\lambda^2 E_b}{+\sigma_\eta^2}\right) p(\lambda)d\lambda, \qquad (7.4.11)$$

$= E_x$ is the mean signal power per
function of the singular values λ_k in
By taking the bandwidth expansion
, the BER of the MC coded OFDM

$$\left.\frac{N}{(N+\bar{\Gamma})}\right) p(\lambda)d\lambda. \qquad (7.4.12)$$

ve the exact BER expression due
(7.4.9) after the inversion of the
ard to derive its lower and upper
ded by the BER when all the K
d., i.e.,

$$\left.\overline{\bar{\gamma})}\right) p(\gamma)d\gamma, \qquad (7.4.13)$$

λ_k in (7.4.10) as

(7.4.14)

of random variable γ. The
total noise power of all the
ts in $(V_k(n))^{-1}\tilde{\xi}_k(n)$, i.e.,

$$) p(\gamma)d\gamma, \qquad (7.4.15)$$

tion of the singular values
$_k(n)$ are Rayleigh fading.
ermined as follows, when

Theorem 7.1 *The distribution of the singular values of a vector OFDM system, i.e., $K = N$, in frequency-selective multipath Rayleigh fading channels is Rayleigh distribution.*

Proof. The blocked channel $\mathbf{H}(z)$ in Fig.7.4 of $H(z)$ has the diagonalization (2.3.10). By (7.2.9), $\mathbf{H}_k = \mathbf{H}(z)|_{z=\exp(j2\pi k/N)}$, the singular values of $\mathbf{H}_k$ are the magnitudes of $H(zW_M^m)|_{z=\exp(j2\pi k/(MN))}$ for $m = 0, 1, ..., M-1$. Since each coefficient $h_l(\frac{NM}{2})$ in $H(z)$ is complex Gaussian, the random variables $H(zW_M)|_{z=\exp(j2\pi k/(MN))}, k = 0, 1, ..., N-1$ are also complex Gaussian. This proves Theorem 7.1. ■

Notice that when $M = 1$, the vector OFDM is the conventional OFDM and therefore, the singular values of the conventional OFDM systems also have the Rayleigh distribution.

Theorem 7.2 *The distribution of the singular values of an MC coded OFDM system with $K = 1$ in frequency-selective multipath Rayleigh fading channels is Nakagami distribution.*

Proof. From the proof in Theorem 7.1, all components in each matrix $\mathbf{H}_k$ are all complex Gaussian. When $K = 1$, the singular values of $\bar{\mathbf{H}}_k$ are the norms of the the first columns of matrix $\mathbf{H}_k$, which, therefore, has Nakagami distribution. ■

For the MC coded OFDM system in (7.2.15) with a general $K < N$, the distribution of the singular values varies between gamma and Nakagami distributions from our many numerical examples. Some examples are shown in Section 7.4.2 and see Fig.7.9 and Fig.7.10.

Since, the BER bounds in (7.4.13) and (7.4.15) depend on γ in (7.4.14) and its probability density function. It is important to estimate it. Although we are not able to analytically prove any distribution result for $K > 1$, our many numerical results show that it is not hard to see the distribution from the histogram of γ as shown in Fig.7.10(b), where it is a gamma distribution.

7.4.2 Simulation Results

We now present some simulation results on the MC coded OFDM system in Fig.7.2 in frequency-selective Rayleigh fading channels. We consider two ray Rayleigh fading channels with equal power, i.e., $L = 2$ and $\Omega_1 = \Omega_2$. Each Rayleigh fading ray is generated by the Jakes's method [127] with the following parameters: 34 paths with equal strength multipath components, 8 oscillators, carrier frequency $f_c = 850$ MHz, simulation time sample interval length $T_s = 41.667\mu s$. The velocities of users considered are

$v = 4$ km/hour, $v = 40$ km/hour and $v = 100$ km/hour. The corresponding Doppler shifts are 3.15 Hz, 31.48 Hz, and 78.7 Hz, respectively.

We first consider the length of the DFT/IDFT in the MC coded OFDM system to be $N = 64$. The channel independent MC (7.2.10) is used. In order to have the same update time duration length, the DFT/IDFT length in the conventional OFDM system is 192 and thus the channel update time duration length is $192T$ for both the MC coded and the conventional OFDM systems. In the decoding, the channel values $h_0(96)$ and $h_1(96)$ are used. In this simulation, the user moving speeds are 4 km/hour and 40 km/hour. Let us first see the singular value distributions, which do not depend on a Doppler shift but on the OFDM block size, the MC size, and the DFT/IDFT size. Fig.7.9 (a) and (b) show the singular value histograms of the conventional OFDM systems and the MC coded OFDM systems with $K = 1$ and $M = 2$, respectively. One can see that the singular values of the conventional OFDM systems have the Rayleigh distribution while the ones of the MC coded OFDM systems have the Nakagami distribution as Theorems 1 and 2 claimed. The singular value histogram of the MC coded OFDM system with $K = 2$ and $M = 3$ is shown in Fig.7.10(a) and it is a gamma distribution. The histogram of

$$\gamma = \frac{1}{\lambda_1^2} + \frac{1}{\lambda_2^2}$$

is shown in Fig.7.10(b), which has gamma distribution too, but with different parameters. It is usually the case that, the larger the singular values are, the better the performance of the OFDM system is. From Figs.7.9-7.10, one can see that the singular value mean of the MC coded OFDM systems with $K = 2$ and $M = 3$ is larger than the ones of the conventional and vector OFDM systems, and the one of the MC coded OFDM system with $K = 1$ and $M = 2$ is larger than the one of the MC coded OFDM system with $K = 2$ and $M = 3$.

In the following BER performance simulations, we consider the MC in (7.2.10) with $K = 2$ and $M = 3$, i.e., the MC coding rate is 2/3. We also consider the conventional convolutionally coded (CC) OFDM with CC rate 2/3 and constraint length 2 and 3×2 generator matrix $[1, 1 + D; 1 + D, D; 1, 1]$. The Viterbi decoding algorithm is used after the OFDM decoding in the COFDM. Fig.7.11(a) and (b) show the performance comparisons when the moving speeds are 40 km/hour and 4 km/hour, respectively.

When the user moving speed is 100 km/hour, we consider the total block size 48: the DFT/IDFT size for the MC coded ($K = 2$ and $M = 3$) and the conventional OFDM systems are 16 and 48, respectively. The reason for reducing the size is that when the Doppler shift is large, the channel update

ır. The corresponding
spectively.
he MC coded OFDM
(7.2.10) is used. In
ne DFT/IDFT length
channel update time
conventional OFDM
and $h_1(96)$ are used.
our and 40 km/hour.
hich do not depend
e MC size, and the
value histograms of
FDM systems with
e singular values of
stribution while the
ami distribution as
m of the MC coded
.7.10(a) and it is a

too, but with dif-
he singular values
s. From Figs.7.9-
MC coded OFDM
f the conventional
ed OFDM system
IC coded OFDM

nsider the MC in
rate is 2/3. We
OFDM with CC
rix $[1, 1+D; 1+$
e OFDM decod-
nce comparisons
respectively.
r the total block
$M = 3$) and the
The reason for
channel update

needs to be faster in order to maintain a certain system performance quality. The channel update time duration length in both systems is $48T_s$. The BER performances of the MC coded OFDM and the COFDM are shown in Fig.7.12(a). One can see that the BER performances of the MC coded and the convolutional coded OFDM systems are comparable while the decoding of the MC coded OFDM system is much simpler than the Viterbi decoding in the COFDM. The performances of the MC coded OFDM and the conventional COFDM, however, differ significantly when the spectral-null time-invariant ISI channel is considered as shown in Fig.7.12(b).

As a remark, although we only showed results in Rayleigh fading channels with two equal power rays, similar results hold with more than two rays.

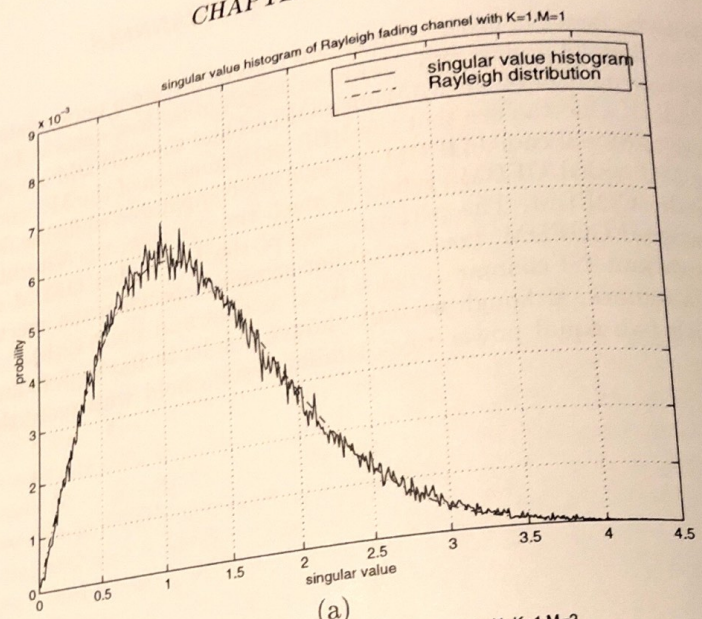

(a)

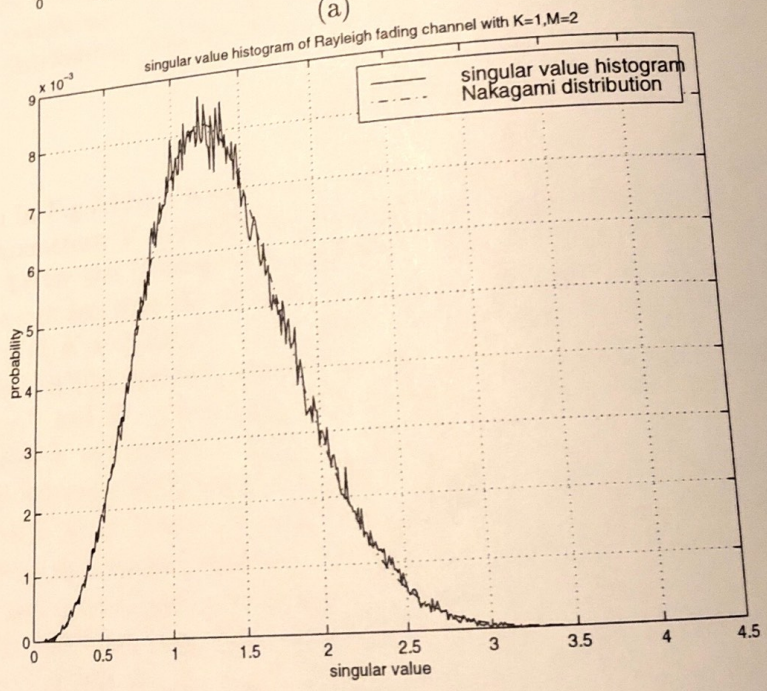

(b)

Figure 7.9: Singular value histograms of the conventional and MC coded OFDM systems in a two ray frequency-selective Rayleigh fading channel: (a) $K = 1$ and $M = 1$; (b) $K = 1$ and $M = 2$.

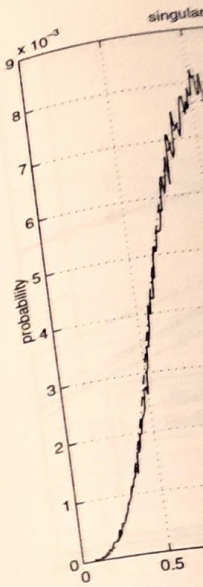

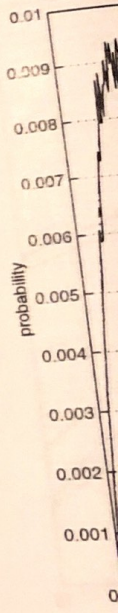

Figure 7.10
$K = 2$ and
(a) singula

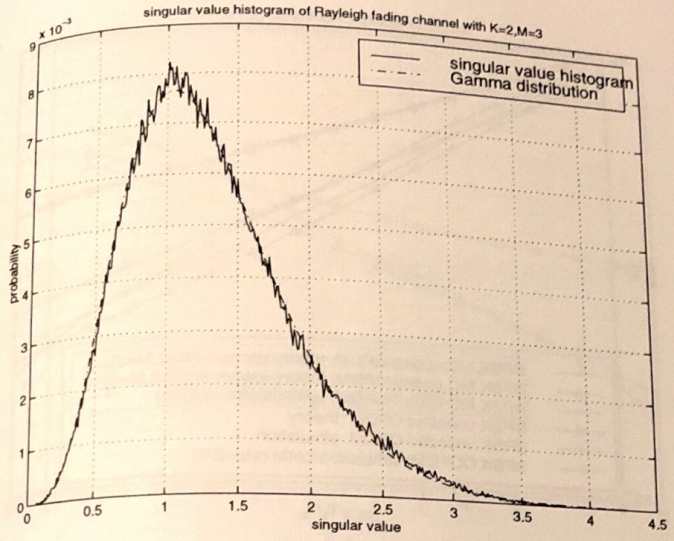

(a)

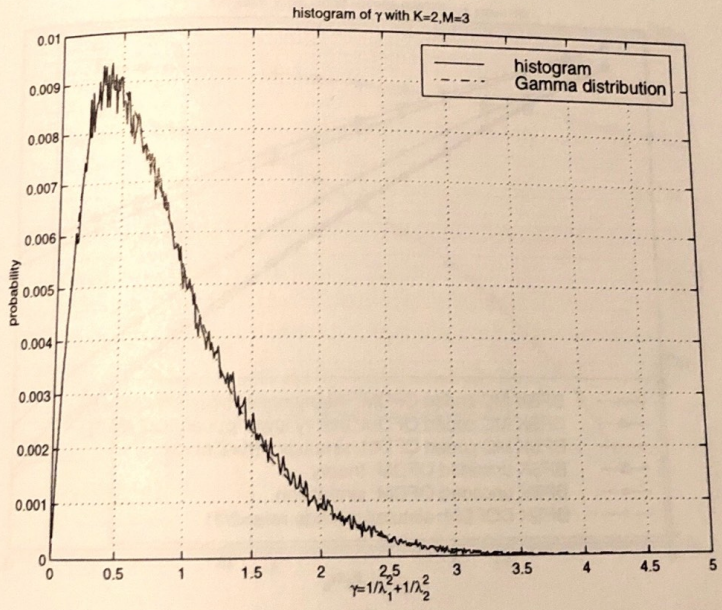

(b)

Figure 7.10: Singular value histograms of MC coded OFDM systems with $K = 2$ and $M = 3$ in a two ray frequency-selective Rayleigh fading channel: (a) singular value historgram; (b) γ histogram.

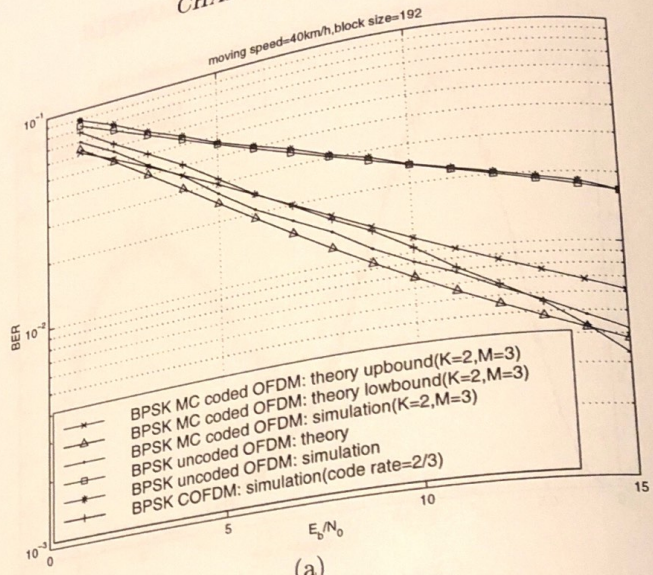

(a)

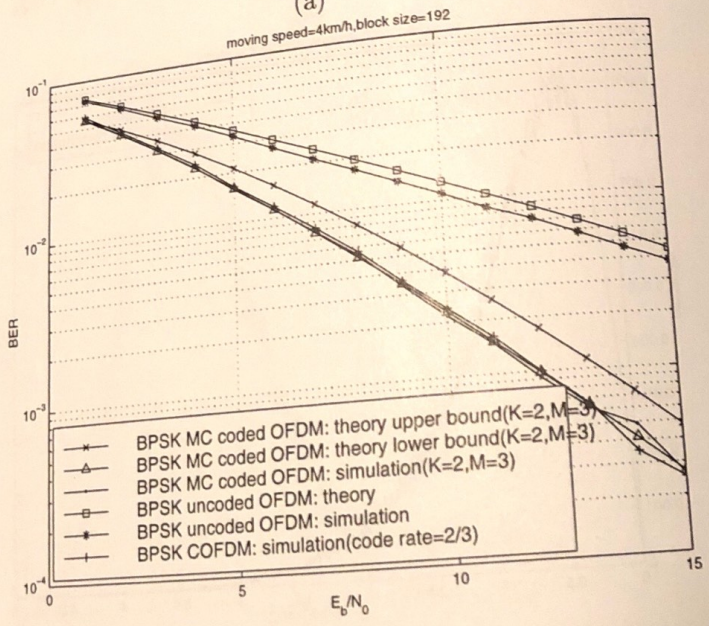

(b)

Figure 7.11: Performance comparison of the conventional OFDM, MC coded OFDM, and COFDM systems in two ray frequency-selective Rayleigh fading channels with moving speed (a) 40km/h and (b) 4km/h.

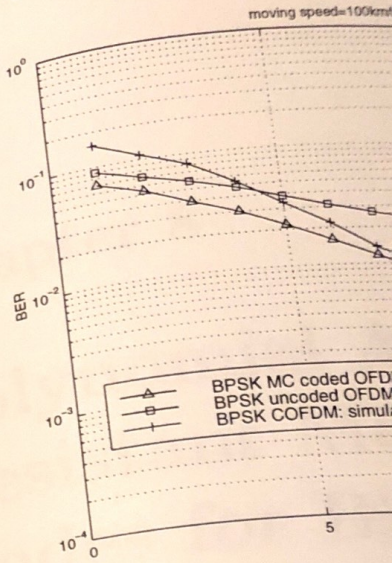

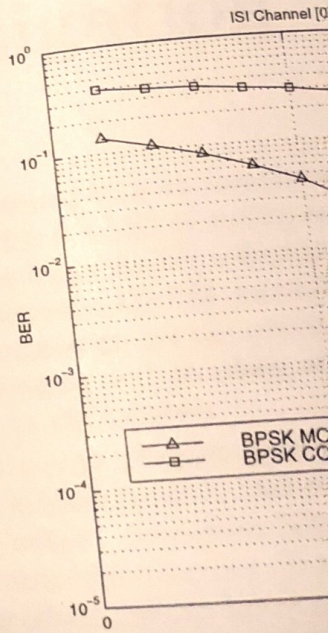

Figure 7.12: Performance
systems in (a) two ray fr
moving speed 100km/h a

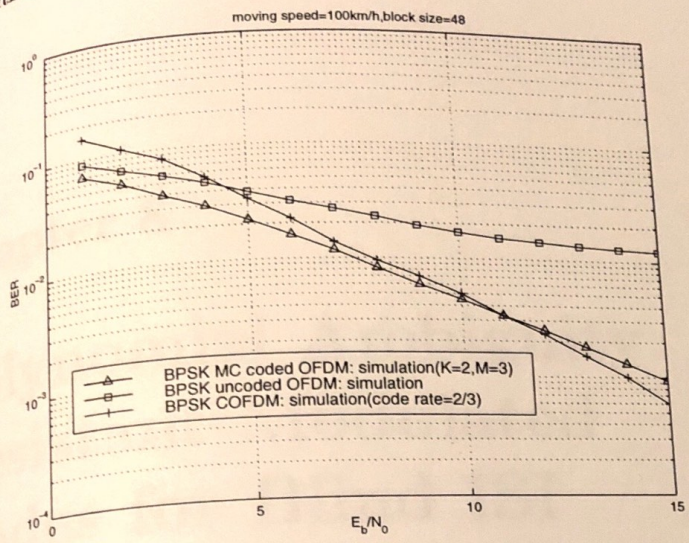

(a)

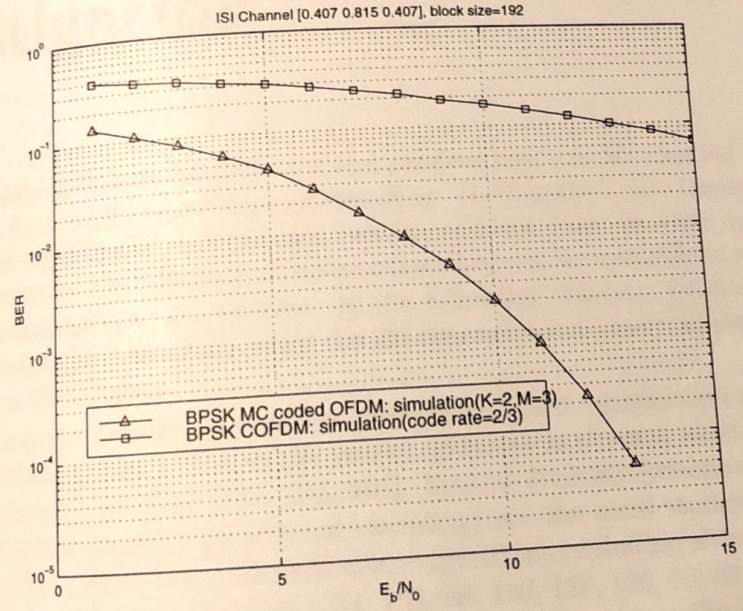

(b)

Figure 7.12: Performance comparison of MC coded OFDM and COFDM systems in (a) two ray frequency-selective Rayleigh fading channels with moving speed 100km/h and (b) spectral-null ISI channel.